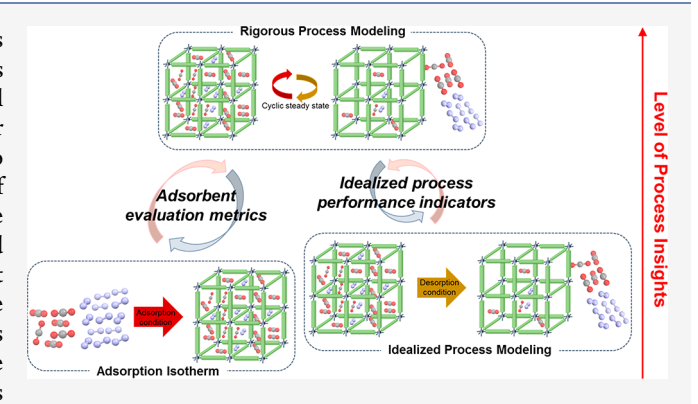


How Well Do Approximate Models of Adsorption-Based CO₂ Capture Processes Predict Results of Detailed Process Models?

Jongwoo Park, [†] Héctor Octavio Rubiera Landa, [†] Yoshiaki Kawajiri, ^{†,‡} Matthew J. Realff, [†] Ryan P. Lively, [†] and David S. Sholl*, [†]

Supporting Information

ABSTRACT: Appropriate selection of adsorbent materials is essential in developing adsorption-based processes such as CO₂ capture. Approximate methods to evaluate material candidates exist using adsorbent evaluation metrics or simplified process models. These approximate methods do not, of course, completely describe the performance of adsorbents in real separation processes. Here, we assess the correlations between approximate predictions and detailed process models of pressure swing adsorption (PSA) at subambient temperatures for postcombustion CO₂ capture using metal—organic frameworks (MOFs). Our results indicate that CO₂ swing capacity and adsorbent performance score are useful in predicting the ranking of materials for this



process. These results illustrate the opportunities and challenges in bridging approximate and detailed methods for evaluating adsorbents for cyclic separations processes.

1. INTRODUCTION

Atmospheric CO₂ concentrations are rising due to anthropogenic emissions. 1,2 This has motivated efforts to develop cost-effective and energy-efficient carbon capture processes. Cyclic adsorption-based CO₂ capture has emerged as a promising approach. Typical examples of these processes include pressure swing adsorption (PSA), vacuum swing adsorption (VSA), and temperature swing adsorption (TSA).4-7 Adsorption-based carbon capture is a materialsenabled technology. Porous materials including activated carbon, zeolites, and metal-organic frameworks (MOFs) have been actively examined for use in CO₂ capture processes.^{2,8-11} Although effective cycle configurations are important, the performance of cyclic adsorption processes depends heavily on the selection of adsorbent materials. 12 Given the large numbers of potential adsorbents that exist, finding effective means to evaluate adsorbents is a key challenge in developing cyclic adsorption-based CO2 capture processes.

A major hurdle in adsorbent evaluation is the choice of performance descriptors. When a large spectrum of adsorbent materials are screened, single component adsorption isotherms for gas species of interest are typically the only information that can be reasonably obtained.^{7,11} Multiple approximate performance metrics that can readily be calculated from these isotherms have been proposed.^{7,12–18} These metrics are typically based on physical intuition.^{7,12} They have served as proxies to evaluate a wide spectrum of materials, especially

when combined with high-throughput molecular modeling of adsorption isotherms. $^{17-23}$

Another way to predict the performance of an adsorbent for CO_2 capture is to use simplified process models describing fully detailed PSA and/or VSA processes. These models are designed to provide industry-relevant performance descriptors such as product purity and energy consumption without the complexity of detailed process modeling. These models avoid the complexity associated with detailed process optimization and can be used with limited information beyond single component adsorption isotherms. These models do not, however, include detailed cycle configurations, so there is a gap between what they can predict and the performance of real processes.

Several studies have used detailed process optimization in combination with approximate metrics to better understand the suitability of materials for adsorption-based separations. 12,28–34 These studies have primarily focused on a restricted spectrum of materials that satisfy targeted constraints of product purity and recovery. Motivated by these previous contributions, the objective of this article is to directly assess

Special Issue: Carbon Capture and Utilization

Received: September 26, 2019
Revised: December 10, 2019
Accepted: December 18, 2019
Published: December 18, 2019

[†]School of Chemical & Biomolecular Engineering, Georgia Institute of Technology, Atlanta, Georgia 30332, United States ‡Department of Materials Process Engineering, Nagoya University, Furo-cho 1, Chikusa, Nagoya 464-8603, Japan

the capability of simple proxies for adsorbent performance and approximate models of cyclic adsorption to predict the outcomes of detailed process models of adsorption-based CO_2 capture processes. We consider the situation where a range of adsorbent materials is available and each level of modeling is used to rank the materials in terms of performance. After producing these rankings with models of multiple levels of complexity and fidelity, it is possible to discuss the correlations between predictions from the simpler models and detailed process models.

We focus below on the use of MOFs as adsorbents for subambient PSA for postcombustion CO₂ capture. Subambient separations have been recently reported by Air Liquide for large-scale CO2 separation from power plant flue gas via a membrane system, which appeared feasible when implemented with appropriate heat integration and power recovery. 35-37 A potential advantage of operating a PSA process at subambient temperatures is the ability to achieve large swing capacities for adsorption. We previously examined a large number of MOFs with respect to this metric and showed that many materials exist with a CO₂ swing capacity larger than 10 mol/kg.³⁸ Below, we use the task of ranking materials of this type for use in subambient temperature CO₂ capture as an example to explore the correlation (or lack of correlation) between predictions based on simplified models and detailed process optimization.

2. METHODS

2.1. Subambient PSA Process. We focus on an adsorption-based PSA CO₂ capture process at subambient temperatures using MOF materials. Unlike many PSA applications where the desired product is the weakly adsorbed molecule in the gas mixture, in treating postcombustion flue gas the aim is to capture the strongly adsorbing species (CO₂).²⁸ In our earlier work,³⁸ the viability of the subambient PSA process using MOFs was estimated using single component CO₂ adsorption isotherms obtained from molecular modeling. Compelling evidence exists that molecular modeling can accurately predict the adsorption isotherms of CO₂ and similar species in a wide range of MOFs. 11,38,39 The large pore volumes and surface areas of MOFs, coupled with a suggested process design made them appealing materials as adsorbents. 6-11,38 Here we extend our focus to a bulk mixture of CO₂/N₂ at compositions relevant to postcombustion flue gas. Real flue gas contains other contaminants including H_2O , O_2 , CO, SO_x , NO_x , and Hg species.^{40–43} The presence of these contaminants could impact adsorption properties of primary components and the stability of adsorbents. 44-46 Air Liquide has demonstrated that dry flue gas feeds can be achieved by appropriate system design combined with a subambient heat exchanger. 47 We therefore focus on adsorptive separation of CO₂ from a dry bulk binary mixture of CO₂/N₂ with molar composition 0.14/0.86 with no other components. We do not have sufficient information to accurately predict the impact of trace impurities such as SO_x and NO_x. Understanding the effects of these kinds of impurities (or mitigating these effects) will be an important step in the practical implementation of any CO₂ capture process. Typical pressures for PSA desorption and adsorption are 0.7 bar ($P_{\text{CO}_2,\text{des}} = 0.1$ bar) and 14.3 bar $(P_{\rm CO_2,ads}=2.0 \text{ bar})$, respectively, at T=243 K. The choice of the pressure swing range and temperature are adapted from earlier findings. 35,36,38 The adsorption and desorption pressures are treated as decision variables in our detailed process models.

2.2. Adsorbent Evaluation Metrics. To evaluate materials as adsorbents for gas capture, a general starting point is to obtain adsorption isotherms for the gases of interest. Multiple efforts have focused on proposing performance metrics that can be derived from adsorption isotherms to forecast their capabilities in end-use applications. Table 1 summarizes the metrics used below to make predictions about PSA processes. 1,13,16

Table 1. Definitions of Adsorbent Evaluation Metrics 7,13,16 Used To Assess Adsorbent Materials 52,53 for Postcombustion $\rm CO_2$ Separation with a Subambient PSA Process

adsorbent evaluation metric		metric formula		
$\Delta N_{ m CO_2} \ m (mol/kg)$	swing capacity	$\Delta N_{\rm CO_2} = N_{\rm CO_2}^{\rm ads} - N_{\rm CO_2}^{\rm des}$		
$S_{ m ads,CO_2/N_2}^{ m ads}$	adsorption selectivity	$S_{\text{ads,CO}_2/N_2}^{\text{ads}} = \frac{N_{\text{CO}_2}^{\text{ads}}/N_{\text{N}_2}^{\text{ads}}}{y_{\text{CO}_2}/y_{\text{N}_2}}$		
$S_{\mathrm{SP,CO_2/N_2}}$	sorbent selection parameter	$S_{\text{SP,CO}_2/N_2} = \frac{(S_{\text{ads,CO}_2/N_2}^{\text{ads}})^2}{(S_{\text{ads,CO}_2/N_2}^{\text{des}})^2} \frac{\Delta N_{\text{CO}_2}}{\Delta N_{\text{N}_2}}$		
$\begin{array}{c} APS_{CO_2/N_2} \\ (mol/kg) \end{array}$	adsorbent performance score	$\mathrm{APS_{CO_2/N_2}} = S_{\mathrm{ads,CO_2/N_2}}{}^{\mathrm{ads}} \Delta N_{\mathrm{CO_2}}$		
R (%)	regenerability	$R = \frac{\Delta N_{\rm CO_2}}{N_{\rm CO_2}} \times 100$		

The first two metrics are the swing capacity and adsorption selectivity.^{7,27} Swing capacity is defined as the difference between the gas storage capacities of the species targeted for capture at the adsorption $(N_{CO_2}^{ads})$ and desorption $(N_{CO_2}^{des})$ pressures chosen as bounds on the process. We computed the CO₂ swing capacity from the difference in CO₂ capacity for a CO₂/N₂ 0.14/0.86 bulk binary mixture at partial pressures for CO₂ of 2.0 and 0.1 bar. The mixture adsorption selectivity is defined as the ratio of adsorption capacity of each component and mole fraction of each component in the bulk phase (y_i) at the adsorption pressure, $P_{\text{total,ads}} = 14.3$ bar (to define $S_{\text{ads,CO}_2/N_2}^{\text{ads}}$) or at the desorption pressure, $P_{\text{total,des}} = 0.7$ bar (to define $S_{\mathrm{ads,CO_2/N_2}}^{\mathrm{des}}$). The next two metrics, the sorbent selection parameter and the adsorbent performance score, combine information from the swing capacity of the component of interest and of the competing species, and the adsorption selectivity at adsorption and desorption pressures under adsorption conditions in different ways. 7,12,16 Such metrics aim to reflect the trade-off relationships that generally exist between swing capacity and adsorption selectivity. 48,49 A remaining metric, the regenerability, is the ratio of the swing capacity and the adsorbed amount of strongly adsorbed species at the adsorption pressure. This parameter estimates the fraction of the adsorption sites that are regenerated during the desorption step. 18,19 All adsorbent evaluation metrics above are calculated from mixture adsorption data (N_i) . $^{7,13,17-19}$ In principle, the molar composition of the bulk phase at the desorption condition completely describes the amount of adsorbing molecules at the desorption pressure (N_i^{des}) . Estimating information regarding the desorption condition is, however, complicated because defining the composition of the

bulk phase is not trivial. 12,50 Hence relying on adsorption conditions as described above has been a common practice. 7,13,17-21

We obtained mixture adsorption data using molecular modeling via Grand Canonical Monte Carlo (GCMC) simulations. The MOFs of interest were taken from a subset of the CoRE MOF database, 51 namely, the energy optimized CoRE MOF DDEC charge database, \$2,53 which includes 477 DFT optimized structures to which high-quality atomic point charges have been assigned. A total of 143 MOFs were selected from this collection that showed PSA CO2 swing capacity exceeding 4 mol/kg at 243 K between 0.1 and 2.0 bar. 38 Binary mixture GCMC simulations were conducted in these 143 materials to calculate adsorption properties of a CO₂/N₂ mixture at bulk pressures of 0.7 and 14.3 bar. The resulting mixture adsorption properties were then used to calculate the adsorbent evaluation metrics in Table 1 for each material. Detailed descriptions of the molecular modeling and the materials we used are given in the Supporting Information (sections S1 and S2).

2.3. Idealized PSA Process Model. Adsorbent evaluation metrics do not necessarily translate into process-level insights. Several simplified adsorption process models have been proposed to overcome this limitation. 24-27 Such models impose multiple assumptions on adsorbents and cycle configurations but are analogous to cyclic adsorption processes. We adapted an idealized PSA process model proposed by Ga et al.²⁷ because it is perhaps the simplest model to implement. This model provides two process performance indicators for an idealized ad-/desorption cycles, namely product purity (Puco,) and specific energy consumption (En_{CO2}). The latter quantity provides insight into the separation cost. In addition, swing capacity ($\Delta N_{\rm CO_2}$ and/or $\Delta N_{\rm N_2}$) can be obtained separately. In this idealized model the compositions of the gas products are found by numerically solving a series of nonlinear equations of mixture adsorption capacities. The major assumptions underlying this idealized description of PSA are that the process operates isothermally without dispersion or kinetic effects with a two-step cycle configurations for ad-/desorption and that adsorption is described as a binary mixture of a strongly and a weakly adsorbing species. The model assumes the use of a compressor and vacuum and also assumes 100% product recovery is achieved. The idealized PSA process is illustrated in Figure 1.

A fundamental piece of information to perform process modeling is the mixture adsorption equilibrium. The model outlined above requires an analytical expression or other methods to estimate the mixture adsorption equilibrium at different pressures, temperatures, and mole fractions in the gas phase. ^{12,54} We employed ideal adsorbed solution theory (IAST) ^{54–56} to predict mixture adsorption. IAST estimates the mixture equilibrium from single component adsorption isotherms by assuming an ideal solution is formed by the adsorbed phase. ⁵⁵ We simulated single component adsorption isotherms for CO₂ and N₂ at temperatures of 213, 228, 243, 258, and 273 K via GCMC. More details of the idealized PSA process model and IAST are given in the Supporting Information (Section S4).

2.4. Rigorous Process Model. Due to the inherent complexity of cyclic adsorption processes, detailed process optimization modeling is needed to achieve the highest fidelity regarding the evaluation of adsorbent materials. We used a

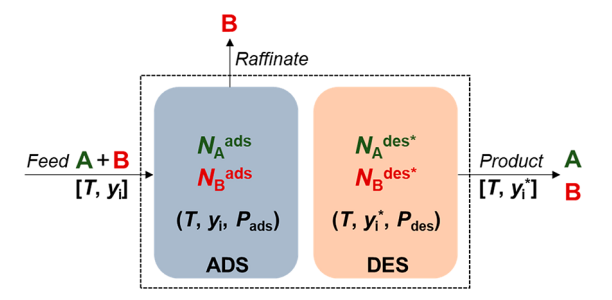


Figure 1. Schematic illustration of the idealized PSA process model. The model imposes idealized cycle of adsorption (ADS) and desorption (DES) with feed binary mixture of CO_2/N_2 in molar fraction of 0.14/0.86 (y_i) . Components A and B refer to strongly and weakly adsorbing species, respectively. The model numerically solves for the composition of the produced gas or molar composition of gas components in the desorption step (y_i^*) . Adsorption amounts at given desorption conditions can be obtained $(N_i^{\text{des}*})$. Isothermal operation is assumed at T=243 K.

rigorous process model with multiobjective optimization^{57,58} to assess the cyclic performance of each MOF considered. Table 2 summarizes the definitions used for our process-level objectives.

Table 2. Definitions of Process-Level Objectives from Multiobjective Optimization Used To Assess Adsorbent Materials for Postcombustion ${\rm CO}_2$ Separation with a Subambient PSA Process

objectives	objective formula		
purity, Pu _{CO2} (%)	$Pu_{CO_2} = \frac{total\ CO_2\ moles\ in\ the\ extract\ product}{total\ gas\ moles\ in\ the\ extract\ product}\times 100$		
recovery, Re _{CO₂} (%)	$\mathrm{Re}_{\mathrm{CO}_2} = \frac{\mathrm{total}\; \mathrm{CO}_2\; \mathrm{moles}\; \mathrm{in}\; \mathrm{the}\; \mathrm{extract}\; \mathrm{product}}{\mathrm{total}\; \mathrm{CO}_2\; \mathrm{moles}\; \mathrm{fed}\; \mathrm{into}\; \mathrm{the}\; \mathrm{cycle}} \times 100$		
$\begin{array}{c} productivity, \\ Pr_{CO_2} \\ [mol/(kg\cdot s)] \end{array}$	$Pr_{CO_2} = \frac{total\ CO_2\ moles\ in\ the\ extract\ product}{total\ adsorbent\ mass}\ \times\ cycle\ time$		
energy, En _{CO₂} (kWh/t)	$En_{CO_2} = \frac{\sum_{i=\text{cycle configuration}} E_i}{CO_2 \text{ mass in the extract product per cycle}}$		

We considered a PSA process model based on a four-step Skarstrom cycle. $^{5,59-61}$ Figure 2a illustrates this cycle, which includes light product pressurization 4,58 with N_2 , adsorption of CO₂ and production of N₂, cocurrent blowdown, and countercurrent evacuation with production of CO2. Our model implemented mathematical expressions to describe packed-bed operation of a PSA under non-isobaric conditions. This includes transient balance equations which are a set of nonlinear partial differential equations (PDEs) coupled with molecular diffusion and adsorption properties. The linear driving force model^{4,62} and the mixture adsorption isotherms predicted by IAST are used for molecular diffusion and adsorption properties, respectively. A finite volume method was applied to discretize the PDE system in space by taking account flux function approximations. 63,64 This results in a set of ordinary differential equations (ODEs) that were solved using MATLAB with the ode15s function at default tolerances until the system reaches the cyclic steady state. Details of PSA modeling are provided in section S5 of the Supporting Information.

Industrial & Engineering Chemistry Research

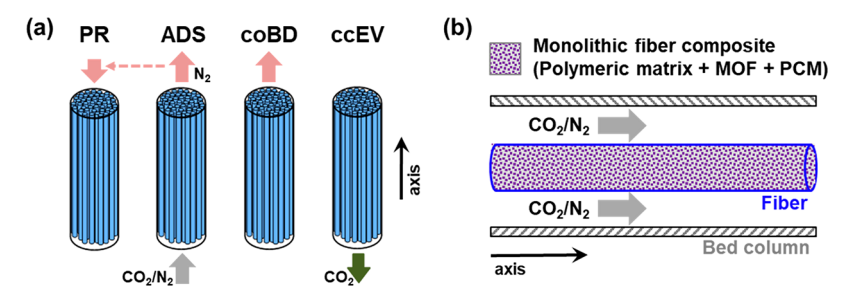


Figure 2. (a) Schematic illustration of the four-step PSA cycle for the rigorous process modeling of a thermally-modulated fiber composite bed contactor. The cycle includes counter-current light product pressurization (PR), adsorption (ADS), cocurrent blowdown (coBD), and counter-current evacuation (ccEV). (b) Schematic illustration of the PCM-based fiber composite and flow of bulk CO_2/N_2 mixture in the bed column.

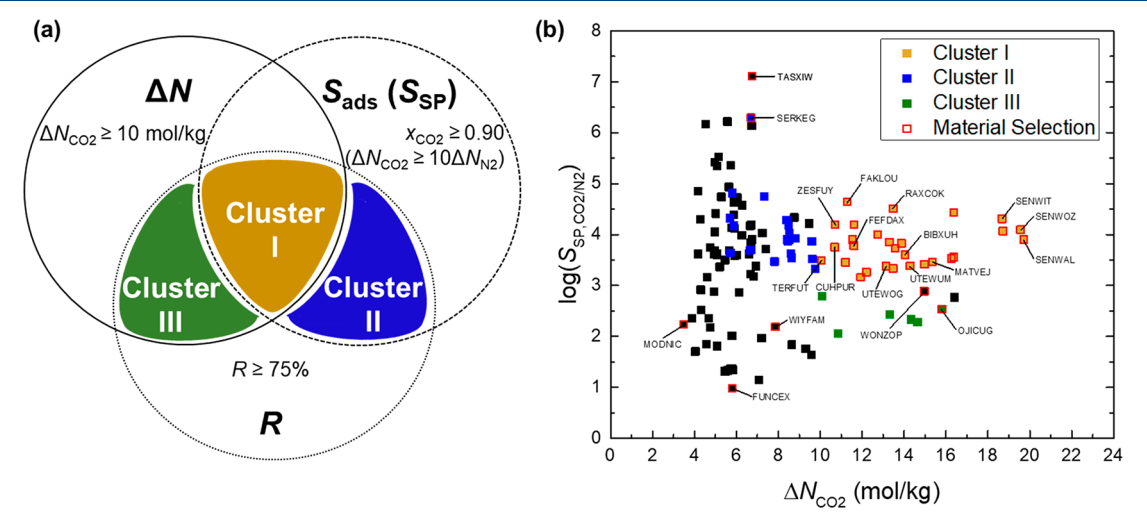


Figure 3. (a) Material selection strategy employed in this work to filter 143 MOFs by forming clusters. The constraints on each metric and definitions of each cluster are described in the text. (b) Adsorbent evaluation metrics calculated for a CO_2/N_2 0.14/0.86 mixture at bulk pressures of 0.7 and 14.3 bar at 243 K. The horizontal and vertical axes are the swing capacity and the sorbent selection parameter, respectively. Data in black squares correspond to MOFs that do not belong to any of the clusters we defined.

Our rigorous process model focused on thermally modulated fiber composite adsorbents, as illustrated in Figure 2b. 65-70 Incorporation of fiber adsorbents as structured contactors in cyclic adsorption processes allows for efficient mass and heat transfer and reduced pressure drop relative to packed beds. 71-74 We modeled a fiber adsorbent contactor composed of a non-adsorbing polymeric matrix, MOF particles, and microencapsulated phase change materials (PCM).65-67 Judicious use of PCM can enable near-isothermal operation of a PSA by its melting and freezing upon CO2 adsorption (exothermic reaction) and desorption (endothermic reaction).⁷⁴ By assuming this approach for heat management, we modeled the process as allowing temperature variation modulated with PCM. Details of the modeling of fiber adsorbent are available in the Supporting Information (Section S5). Only the PSA unit is considered in this work without assessing other details of the flowsheet that would be required to completely describe an integration of this unit with a power plant.

Subambient PSA process modeling above was coupled with multiobjective optimization. Optimization was carried out in MATLAB using the *gamultiobj* function for which a variant of the NSGA-II genetic algorithm sa, was applied. We consider the rigorous process modeling as a black-box function with a set of available decision variables as inputs and process-level objectives at cyclic steady state as outputs. Further details of the optimization procedures are provided in the Supporting

Information (Section S5). This optimization leads to maximizing purity, recovery, and productivity while minimizing energy consumption under each process condition that is determined by decision variables.

3. RESULTS AND DISCUSSION

3.1. Adsorbent Evaluation by Approximate Models. It is typically impractical to conduct rigorous process modeling or to perform detailed experimental testing for hundreds of potential adsorbent materials. We therefore used approximate models to reduce the number of MOFs to examine with our detailed process model. We began by examining 143 MOFs using the adsorbent evaluation metrics in Table 1 and then studied 35 of these adsorbents using the idealized PSA process model described in section 2.3. The goal of this work was not to identify individual "winning" materials but to reveal a spectrum of materials performance that could then be compared for selected materials to our more rigorous process model.

3.1.1. Material Selection by Adsorbent Evaluation Metrics. A total of 143 MOFs were characterized with the adsorbent evaluation metrics in Table 1. In order to discover high-performing materials, previous studies commonly used one or two of the metrics in Table 1.^{7,13–21,38} Top-ranked materials for a single metric^{7,13,21,38} or those judged to have a good combination of each metric^{17–19} were then labeled as potential adsorbents. We employ the latter screening strategy

Industrial & Engineering Chemistry Research

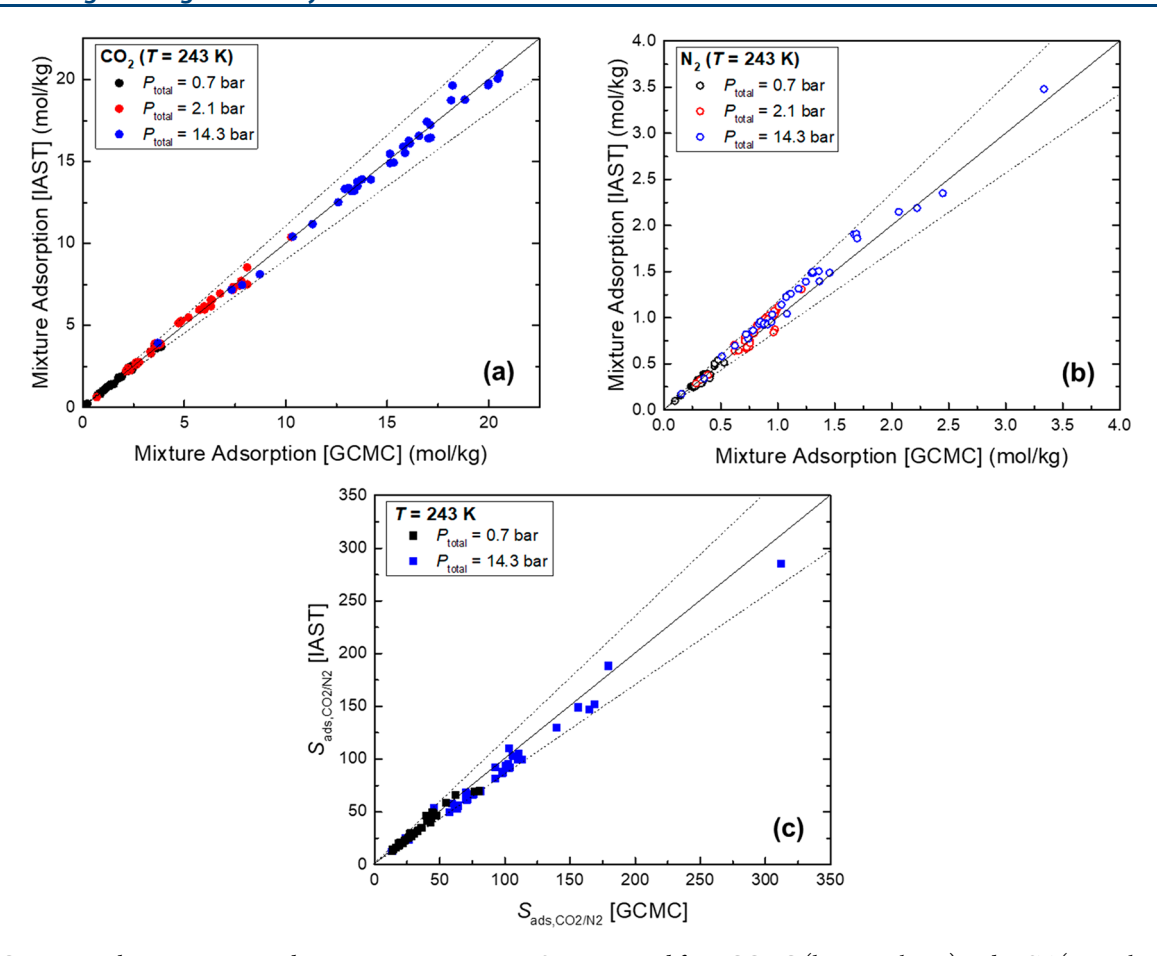


Figure 4. Comparison between mixture adsorption amounts in 35 MOFs computed from GCMC (horizontal axes) and IAST (vertical axes) for (a) CO_2 and (b) N_2 at low, intermediate, and high total pressures at 243 K and (c) adsorption selectivities in 35 MOFs computed from GCMC (horizontal axis) and IAST (vertical axis). In all cases the gas phase CO_2/N_2 composition is 0.14/0.86. The diagonal lines have slopes of 1.1, 1, and 0.9 from top to bottom, respectively, in (a). Similar lines are drawn for slopes of 1.15, 1, and 0.85 from top to bottom, respectively, in (b) and (c).

for the filtering of MOF candidates. Our strategy is illustrated in Figure 3a.

We first set constraints for each metric. A key advantage of subambient gas processing is that the swing capacity for small molecules can be large.³⁸ On this basis the lower bound for swing capacity was set to 10 mol/kg. Adsorption selectivity has long been viewed as controlling the achievable product purity. 4,20 We set a lower bound on the mole fraction of CO_2 in adsorbed phase (x_{CO_2}) of 0.9 when considering selectivity. The sorbent selection parameter includes information from the swing capacities for both CO₂ and N₂. Increasing or suppressing the adsorption of strongly or weakly adsorbing molecules, respectively, is a route for efficient separation of gas mixtures. 13,20,24,33 We therefore set a constraint to have $\rm CO_2$ swing capacity more than ten times the N2 swing capacity. The adsorbent performance score is calculated by the product of swing capacity and adsorption selectivity. We use same constraints of swing capacity and adsorption selectivity when setting the constraint for this quantity. Having a highly selective adsorbent does not guarantee high regenerability. We adopted a target regenerability of 75% from previous work. 18 The "best" adsorbents at this stage would be candidates that meet all of these constraints (cluster I in Figure 3a). To ensure we are considering a spectrum of materials, we also considered materials that satisfy some but not all of these constraints. Figure 3a indicates clusters of materials that have extremely high selectivity but relatively low swing capacity (cluster II) or vice versa (cluster III in Figure 3a). In order to make our discussion more robust, we also included several MOFs that are not categorized in any of the clusters we defined above. These MOFs were randomly chosen from the set of materials that do not meet the constraints for any combination of the metrics above.

Figure 3b shows the adsorbent evaluation metric data for 143 MOFs and clustering of this information as defined in Figure 3a. Twenty-eight MOFs were found from cluster I. We then selected additional MOFs from clusters II and III. The swing capacity for CO2 in MOFs from cluster II ranges between 6 and 9 mol/kg, values considerably higher than typical materials for CO2 capture via PSA at ambient temperatures. 76,77 The MOF from cluster II (CSD reference code SERKEG) with the highest sorbent selection parameter was chosen for further consideration. Similarly, the MOF from cluster III (OJICUG) with the largest swing capacity was chosen. Lastly, five additional MOFs that lie outside these clusters (FUNCEX, MODNIC, TASXIW, WIYFAM, and WONZOP) were randomly selected. This defined a set of 35 MOFs that are predicted to have a diverse range of performance characteristics as predicted by the adsorbent evaluation metrics, which were used in our more detailed models. These materials are indicated with highlighted borders in Figure 3b. Information about selected physical properties of

Industrial & Engineering Chemistry Research

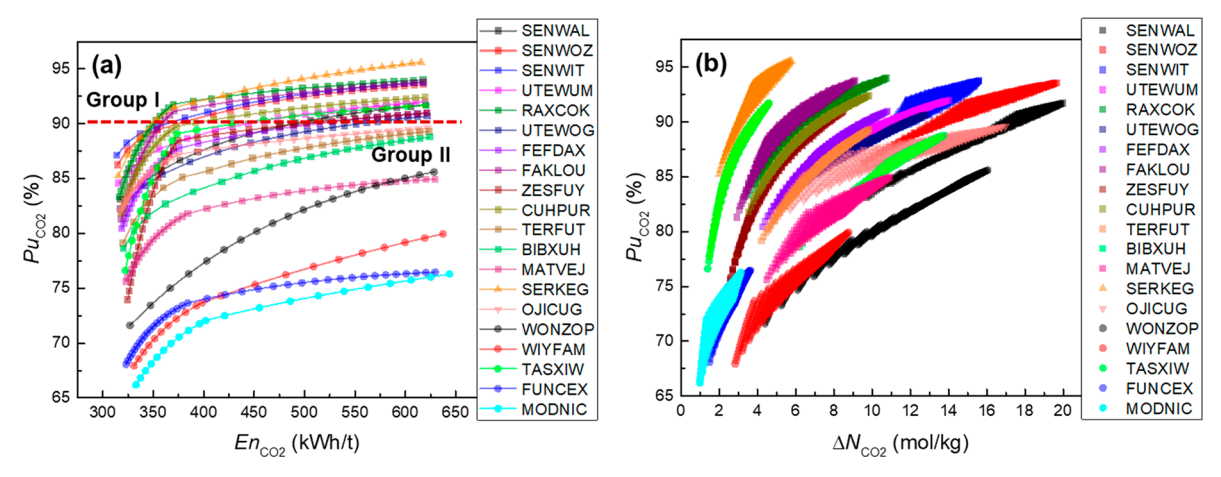


Figure 5. Performance indicators derived from the idealized PSA process model for 20 MOFs. The indicators were calculated for a CO_2/N_2 0.14/0.86 mixture at 243 K for 400 combinations of ad-/desorption pressures. Squares, triangles, downward-pointing triangles, and circles indicate MOFs collected from cluster I, cluster II, cluster III, and nonclustered MOFs, respectively, from the preselection stage. (a) $En_{CO_2}-Pu_{CO_2}$ shown by Pareto fronts across operating pressures in each material. MOFs in group I are the ones that meet the Pu_{CO_2} benchmark while those in group II do not. (b) $\Delta N_{CO_2}-Pu_{CO_2}$ shown with each data points calculated from all combinations of ad-/desorption pressures.

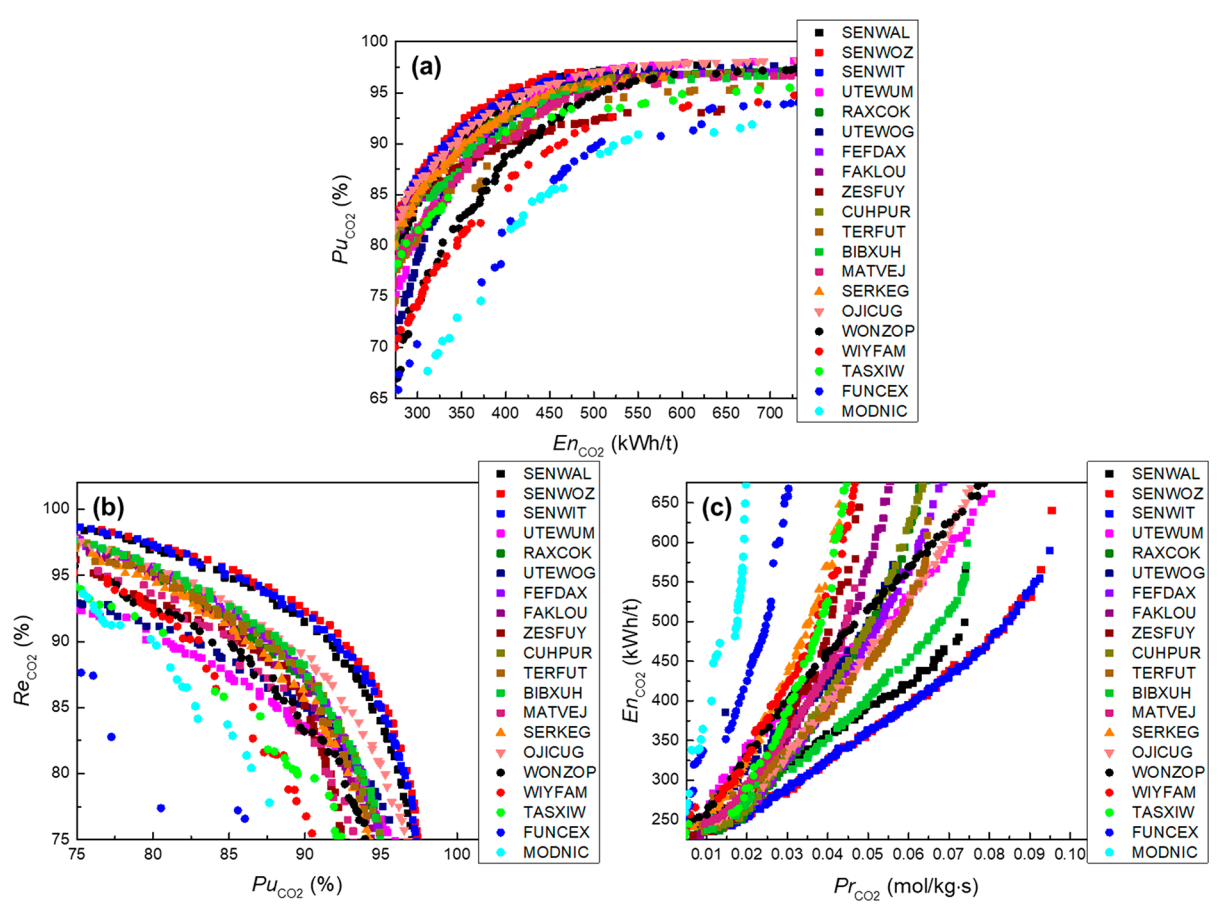


Figure 6. Multiobjective optimization for 20 MOFs in a subambient PSA using a hollow fiber adsorbent module at 243 K. Squares, triangles, downward-pointing triangles, and circles indicate MOFs collected from cluster I, cluster II, cluster III, and nonclustered MOFs, respectively, from the preselection stage. Pareto fronts are shown for optimized objectives of (a) En_{CO_2} and Pu_{CO_2} , (b) Pu_{CO_2} and Re_{CO_2} , and (c) Pr_{CO_2} and En_{CO_2} .

28 MOFs from cluster I is given in Figure S2 (section S3 of the Supporting Information).

3.1.2. Material Selection by an Idealized PSA Process Model. We next used the idealized PSA process model defined above²⁷ to obtain process-level performance descriptors of 35 MOFs. This approach allows us to incorporate a range of

adsorption and desorption conditions.^{24,27} The results obtained from this model were used to further reduce the number of MOFs to which we applied a rigorous process model.

Our process modeling uses IAST to predict mixture adsorption.⁵⁴ Although there are indications that applying

IAST in MOFs may be viable, ^{7,55,56} IAST may be inaccurate at high pressure and for weakly adsorbing molecules. ^{20,56} We therefore directly tested IAST in the 35 MOFs we considered by comparison with mixture GCMC calculations, as shown in Figure 4. Both CO₂ (Figure 4a) and N₂ (Figure 4b) show good agreement between direct simulation of mixture adsorption with GCMC and simulation using IAST within the pressure range of our process. We calculated the fractional IAST error, defined as the ratio of the difference between IAST and GCMC results to the GCMC result. ²⁰ For all 35 materials the fractional error in the CO₂ and N₂ uptakes were less than 10% and 15%, respectively. The fractional error for selectivity was also smaller than 15% for every material (Figure 4c). We took this as an indication that using IAST within our process models was an acceptable approximation ^{20,56} within the range of pressures evaluated here.

We used the idealized PSA model to select materials for use in our detailed process model as indicated in Table S1. We first chose MOFs that do not have open-metal sites (OMS) based on previous reports that examined the crystal structures via connectivity analysis for each metal center. 78,79 This choice avoids complications associated with the limited accuracy of generic force fields for molecular simulations of MOFs with OMS. 11,78-81 Among the 25 non-OMS MOFs, we sampled MOFs on the basis of the CO₂ purity predicted by the idealized model, Pu_{CO2}. We set 90% purity as the benchmark for this quantity.⁸² All MOFs that exceed this benchmark for some combination of process conditions, i.e., adsorption and desorption pressures, were selected. In addition, eight MOFs that did not exceed this standard were randomly chosen to ensure our final selection included a spectrum of materials performance. This gave the list of 20 MOFs shown in Figure 5. The process performance indicators for all 35 MOFs are shown in Figure S3.

Figure 5 shows $\Delta N_{\rm CO_2}$, $\rm Pu_{\rm CO_2}$, and $\rm En_{\rm CO_2}$ for each of the 20 MOFs we considered further. It is important to note that the metrics from Table 1 cannot provide any information about the two latter quantities. These indicators were calculated with the idealized process model at 20 adsorption pressures equally spaced from 5.0 to 15.0 bar and 20 desorption pressures equally spaced from 0.15 to 0.35 bar. Figure 5a shows Pareto fronts with respect to $\rm En_{\rm CO_2}$ and $\rm Pu_{\rm CO_2}$ (which we denote below as $\rm En_{\rm CO_2}$ – $\rm Pu_{\rm CO_2}$ for brevity)across this range of operating conditions. As might be expected, there is a trade-off between $\rm Pu_{\rm CO_2}$ and $\rm En_{\rm CO_2}$. Figure 5b shows $\Delta N_{\rm CO_2}$ and $\rm Pu_{\rm CO_2}$ at each of the 400 process conditions we considered. The sensitivity of $\Delta N_{\rm CO_2}$ – $\rm Pu_{\rm CO_2}$ as a function of process pressures is heavily material dependent.

3.2. Adsorbent Evaluation by a Detailed Process Model. The steps above defined a shortlist of 20 MOFs with a spectrum of performance for subambient CO₂ capture as predicted from a series of approximate models. We used rigorous multiobjective process optimization to develop processes based on each of these MOFs. This optimization allows each adsorbent to be coupled with process conditions that maximize their potential. 83–87

Figure 6 shows the Pareto fronts for pairs of process-level objectives. Figure 6a shows minimization of En_{CO_2} and maximization of Pu_{CO_2} . En_{CO_2} is a useful proxy for operating process cost.⁸⁴ This pair of objectives enables a direct

comparison of the similarities of material evaluation made between the rigorous and idealized process model described in section 3.1.2. Parts b and c of Figure 6 show other common approaches to evaluating the capability of adsorbents and the viability of chosen adsorption system. Figure 6b assesses maximization of Pu_{CO_2} and Re_{CO_2} . We find the presence of MOFs in this subambient system approaching 90% and 95% for both Pu_{CO_2} and Re_{CO_2} , respectively, a suggested target 82 for these objectives. Figure 6c assesses maximization of Pr_{CO_2} and minimization of En_{CO_2} . This is useful because it identifies process in which energy consumption is low while the maximum productivity for a given mass (or volume) of adsorbent can be reached. We find MOF candidates capable with Pr_{CO_2} up to $\sim\!0.1$ mol/(kg·s) with $\sim\!200$ kWh/t of En_{CO_2} .

The results from Figure 6 allow us to revisit the evaluation of each MOF. When considering $\rm En_{\rm CO_2}-\rm Pu_{\rm CO_2}$, we ranked MOFs using $\rm Pu_{\rm CO_2}$ at a fixed $\rm En_{\rm CO_2}$ of 400 kWh/t. For $\rm Pu_{\rm CO_2}-\rm Re_{\rm CO_2}$, a ranking was made by the product of $\rm Pu_{\rm CO_2}$ and $\rm Re_{\rm CO_2}$. For $\rm Pr_{\rm CO_2}-\rm En_{\rm CO_2}$, we ranked MOFs using $\rm Pr_{\rm CO_2}$ at a fixed $\rm En_{\rm CO_2}$ of 400 kWh/t. These ranking criteria were chosen to represent the choices that are most likely to be a profitable design for our process within a set of target constraints for the process objectives. These three rankings are summarized in Table 3. We give three separate rankings to emphasize that focusing on

Table 3. Three Rankings of MOFs Based on Multiobjective Process Optimization a

Ranking	MOFs Ranked by					
	(a) <i>Enco2-Puco2</i>	(b) <i>Pu</i> CO2- <i>Re</i> CO2	(c) <i>Pr</i> CO2- <i>En</i> CO2			
1	SENWOZ	SENWOZ	SENWOZ			
2	SENWIT	SENWIT	SENWIT			
3	OJICUG	SENWAL	SENWAL			
4	SENWAL	OJICUG	BIBXUH			
5	SERKEG	BIBXUH	TERFUT			
6	FAKLOU	TERFUT	FEFDAX			
7	FEFDAX	FEFDAX	RAXCOK			
8	RAXCOK	CUHPUR	OJICUG			
9	CUHPUR	RAXCOK	CUHPUR			
10	UTEWUM	ZESFUY	UTEWOG			
11	UTEWOG	SERKEG	<i>FAKLOU</i>			
12	BIBXUH	FAKLOU	MATVEJ			
13	TASXIW	MATVEJ	ZESFUY			
14	MATVEJ	UTEWOG	TASXIW			
15	TERFUT	WONZOP	WONZOP			
16	ZESFUY	UTEWUM	UTEWUM			
17	WONZOP	WIYFAM	SERKEG			
18	WIYFAM	TASXIW	WIYFAM			
19	MODNIC	MODNIC	FUNCEX			
20	FUNCEX	FUNCEX	MODNIC			

"Definitions of each ranking are given in the text. MOFs whose ranking varies by five or more places among two rankings are shown in italics. Example materials described in the text (SERKEG, SENWOZ, SENWIT, and SENWAL) are color coded for easy comparisons across the three rankings.

Rigorous	Adsorbent Evaluation Metrics				1.00	
Process Model	$\Delta N_{\rm CO2}$	S _{ads,CO2/N2} ads	S _{SP,CO2/N2}	APS _{CO2/N2}	R	0.80
En _{CO2} -Pu _{CO2}	0.61	0.59	0.56	0.76	0.13	0.60
Pu _{CO2} -Re _{CO2}	0.66	0.28	0.38	0.47	0.45	0.40
Pr _{CO2} -En _{CO2}	0.69	0.29	0.39	0.50	0.33	0.20 dissimilar 0.00

Figure 7. Spearman's rank-order correlation (ρ) between rankings of 20 MOFs from rigorous process modeling (vertical axis) and adsorbent evaluation metrics (horizontal axis). A general guideline for correlation strength and data interpretation associated with the color coding is provided in detail in Table S3 in the Supporting Information.

different aspects of process performance favors different materials. For instance, a material that is a good candidate when the focus is on product purity may be less attractive when process economics are the dominant concern, and vice versa. The MOF with structure code SERKEG is an example; it is ranked in the top five materials for $\rm En_{\rm CO_2}-\rm Pu_{\rm CO_2}$, 11 of 20 with respect to $\rm Pu_{\rm CO_2}-\rm Re_{\rm CO_2}$, and 17 among the 20 materials with respect to $\rm Pr_{\rm CO_2}-\rm En_{\rm CO_2}$. Some materials, however, are ranked quite consistently in each list. The MOFs with structure codes SENWOZ and SENWIT, for example, are ranked 1 and 2 in every list, and SENWAL is ranked either third or fourth in each list.

3.3. Comparing Approximate and Detailed Models of Adsorption-Based Carbon Capture Process. Having introduced the results from each level of modeling, we now turn to comparing results among these models. We first quantify the similarity of results between our rigorous process model and adsorbent evaluation metrics. We then conduct the same analysis with comparison from rigorous and simplified process models.

3.3.1. Rigorous Process Model and Adsorbent Evaluation Metrics. For the group of 20 MOFs ranked by our rigorous process model (Table 3) we also developed rankings based on each simplified adsorbent ranking listed in Table 1. The latter rankings are listed in Table S4. Spearman's rank-order correlation was used to compare the results from these two different levels of modeling. Spearman's rank-order correlation is a nonparametric measure of statistical dependence between the rankings of two variables that assesses how well the relationship between two variables can be described.^{88,89} A rank-order correlation of 1 indicates perfect correlation between two rankings, a value of 0 indicates no correlation between the two rankings, and a value of -1 occurs if two rankings are perfectly anti-correlated. Spearman's rank-order correlations between each process-level ranking and adsorbent evaluation metrics are shown in Figure 7. There is considerable variation between the various ranking methods. This is consistent with previous findings³⁰⁻³³ that suggested caution must be used in using adsorbent evaluation metrics.

Among the five adsorbent evaluation metrics, $\Delta N_{\rm CO_2}$ and ${\rm APS_{\rm CO_2/N_2}}$ appear to be the most useful proxies for process scale performance in our particular process. $\Delta N_{\rm CO_2}$ showed a comparable similar rank correlation for each of the three process-level rankings. The adsorbent performance score, ${\rm APS_{\rm CO_2/N_2}}$, was the most successful adsorbent evaluation metric when process performance was characterized using energy and purity. ${\rm APS_{\rm CO_2/N_2}}$, was only moderately successful,

however, if the process-level ranking was made on the basis of purity and recovery or productivity and energy. Other separation processes that are highly driven by product purity (e.g., direct air capture of CO_2) might result in different correlations. The other three adsorbent evaluation metrics performed relatively poorly. It might be expected that $S_{\mathrm{SP,CO}_2/\mathrm{N}_2}$ would also be useful because it uses a combination of inputs like $\mathrm{APS_{CO_2/N}_2}$. We found, however, that this metric was dominated by $S_{\mathrm{ads,CO}_2/\mathrm{N}_2}^{\mathrm{ads}}$ for the CO_2 capture process we considered. As a result, the rank correlations of $S_{\mathrm{SP,CO}_2/\mathrm{N}_2}^{\mathrm{ads}}$ and $S_{\mathrm{ads,CO}_2/\mathrm{N}_2}^{\mathrm{ads}}$ were quite similar.

As an aside, a possible reason that some metrics make poor predictions in terms of process-level ranking is that individual metrics only reflect specific features of the cyclic process. ¹⁵ To this end, we formulated a combined adsorbent evaluation metric (CAEM) that incorporates linear combinations of the adsorbent evaluation metrics to balance the contribution of each metric. We analyzed the rank correlations between each process-level ranking and the CAEM ranking. We found that the rank correlation can be moderately improved by using CAEM relative to relying on a single winning metric in all cases we examined. This implies that properly balancing the effect of existing metrics may allow better prediction of process-level performance of materials from simpler models. Details of this approach are provided in section S6.

3.3.2. Rigorous and Idealized PSA Process Models. Following the above analysis, we also quantified the similarity in rankings of materials provided from the rigorous and idealized PSA process models. The rankings derived from the idealized PSA model are listed in Table S7. Unlike the situation for adsorbent evaluation metrics, the predicted process performances for each level of modeling can be compared. Because the idealized model only gives $\rm En_{CO_2}$ and $\rm Pu_{CO_2}$ but not $\rm Re_{CO_2}$ or $\rm Pr_{CO_2}$, it is only possible to directly compare these predictions to the detailed process model for the information in Figure 6a.

Figure 8 compares the process objectives in terms of En_{CO_2} – Pu_{CO_2} from the rigorous and idealized process models. The full process optimization (Figure 6a) gives a narrower range of achievable Pu_{CO_2} than the idealized PSA model results (Figure 5a). Since we are primarily interested in the relative performance of different materials, Figure 8 shows a normalized achievable Pu_{CO_2} at a fixed En_{CO_2} of 400 kWh/t for each level of modeling. The Spearman's rank-order correlation for these two levels of modeling was 0.74. When ranking MOFs with respect to En_{CO_2} – Pu_{CO_2} using the

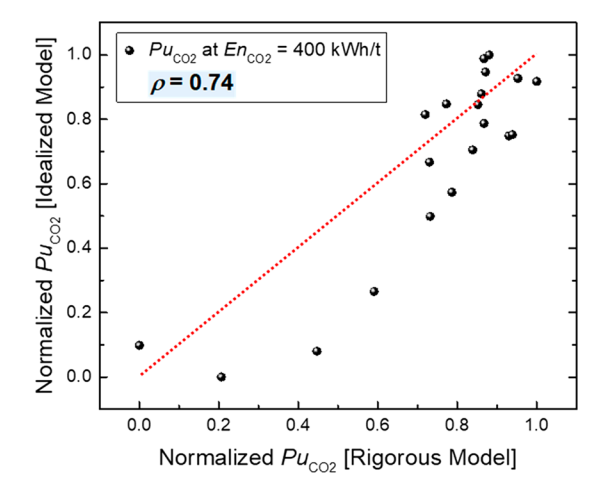


Figure 8. Normalized Pu_{CO2} at a fixed En_{CO2} using results from our rigorous process model (horizontal axis) and an idealized process model (vertical axis). Normalization was performed using the range of values from each data set. The red dashed line is a parity line.

idealized and detailed process models, we compared Puco, at a constraint of En_{CO2}. Because the Pareto fronts are not always on top of each other as a function of En_{CO}, the MOF rankings can vary at different choice of En_{CO2}. We tested the sensitivity of Spearman's rank-order correlation to the choice of En_{CO}, as summarized in Table S8. It is worth noting that we quantitatively compared the rigorous and simplified process predictions using one of several possible simplified models. The rank correlation between two levels of process model may vary depending on which simplified model is used, so testing a range of plausible simplified models would be a useful future extension of this work.

It is also possible to compare the results of the adsorbent evaluation metrics with the idealized PSA process model. A comparison of MOF rankings from these approaches is shown in Figure S5 (section S6 of the Supporting Information). The metrics of adsorption selectivity, sorbent selection parameter, and the adsorbent performance score are strongly correlated with the predictions of the idealized PSA model. Somewhat surprisingly, these are not the same adsorbent evaluation metrics that were best correlated with the predictions from our rigorous process model. At one level, our data suggests that in terms of the ability to rank materials according to their performance as defined by the rigorous process model, the idealized PSA model adds little to the information available from the simpler adsorbent evaluation metrics. This characterization is too simplistic, however, because the idealized model provides information that is not available from the simple metrics (see Figure 5) and the predictive power of the simple metrics is only available when the right metric among multiple possible choices is used.

4. CONCLUSIONS

In this article we examined the value of using approximate models of a subambient PSA process to evaluate a large number of candidate adsorbents for a CO₂ capture process. This work integrates molecular modeling, an idealized process model, and rigorous multiobjective process models to consider a spectrum of materials performance indicators. We examined MOF rankings derived from multiple modeling levels that

allow quantitative measurements on the ranking similarity between approximate and detailed models.

We compared a group of MOFs ranked by rigorous process modeling and adsorbent evaluation metrics. Our findings showed CO₂ swing capacity and the adsorbent performance score of MOFs are successful proxies to predict process-level rankings, while other simple metrics were not as strongly correlated with the detailed results. Our analysis only considered a specific separation process, a PSA process for CO₂ capture from dry flue gas at subambient temperatures, so we cannot conclude that the same two adsorbent evaluation metrics will be the best suited to all possible chemical separations. Nevertheless, the observation that two of the metrics we tested performed far better than the others indicates that future efforts to use adsorbent evaluation metrics in screening libraries of materials should carefully consider which metric(s) are best suited for the process of interest. Our results are an example of the risks that exist if choices about materials selection are made by relying exclusively on a single metric.90 Our models considered the performance of a separations process without regard for many of the practical issues that can limit scale up and implementation of new separations technologies. 91 A useful future extension of this work would be to perform a complete technoeconomic analysis by carefully estimating the capital and operating costs, including assessing the operational lifetime of key components of the cyclic adsorption system. The challenges that almost inevitably arise during this kind of process development mean that making well justified choices at the earliest stages of materials selection and process design are critical. It is hoped that the multilevel modeling approach we have illustrated here can make these choices more reliable and efficient in similar efforts in the future.

ASSOCIATED CONTENT

Supporting Information

The Supporting Information is available free of charge at https://pubs.acs.org/doi/10.1021/acs.iecr.9b05363.

Molecular modeling details; MOF material set; structure-property relationships for adsorbent evaluation metrics; idealized PSA model details and IAST implementation; rigorous process modeling details; comparing approximate and detailed models of adsorption-based carbon capture process; numerical data for analysis (PDF)

Tables included to support the discussion (XLS)

AUTHOR INFORMATION

Corresponding Author

*E-mail: david.sholl@chbe.gatech.edu.

ORCID ®

Jongwoo Park: 0000-0002-8996-8362

Héctor Octavio Rubiera Landa: 0000-0002-9832-4358

Yoshiaki Kawajiri: 0000-0002-7124-1704 Matthew J. Realff: 0000-0002-5423-5206 Ryan P. Lively: 0000-0002-8039-4008 David S. Sholl: 0000-0002-2771-9168

I

The authors declare no competing financial interest.

ACKNOWLEDGMENTS

The authors acknowledge the U.S. Department of Energy through grant DE-FE0026433 for financial support. Any options, findings, conclusions, or recommendations expressed herein are those of the author(s) and do not necessarily reflect the views of the DOE.

REFERENCES

- (1) Mikkelsen, M.; Jorgensen, M.; Krebs, F. C. The Teraton Challenge. A Review of Fixation and Transformation of Carbon Dioxide. *Energy Environ. Sci.* **2010**, *3*, 43–81.
- (2) Choi, S.; Drese, J. H.; Jones, C. W. Adsorbent Materials for Carbon Dioxide Capture from Large Anthropogenic Point Sources. *ChemSusChem* **2009**, *2*, 796–854.
- (3) Sholl, D. S.; Lively, R. P. Seven Chemical Separations to Change the World. *Nature* **2016**, *532*, *435*–437.
- (4) Kikkinides, E. S.; Yang, R. T.; Cho, S. H. Concentration and Recovery of Carbon Dioxide from Flue Gas by Pressure Swing Adsorption. *Ind. Eng. Chem. Res.* 1993, 32, 2714–2720.
- (5) Webley, P. A. Adsorption Technology for CO₂ Separation and Capture: A Perspective. *Adsorption* **2014**, *20*, 225–231.
- (6) Hedin, N.; Andersson, L.; Bergstrom, L.; Yan, J. Adsorbents for the Post-Combustion Capture of CO₂ Using Rapid Temperature Swing or Vacuum Swing Adsorption. *Appl. Energy* **2013**, *104*, 418–433.
- (7) Bae, Y. S.; Snurr, R. Q. Development and Evaluation of Porous Materials for Carbon Dioxide Separation and Capture. *Angew. Chem., Int. Ed.* **2011**, *50*, 11586–11596.
- (8) Ferey, G.; Mellot-Draznieks, C.; Serre, C.; Millange, F. Crystallized Frameworks with Giant Pores: Are There Limits to the Possible? *Acc. Chem. Res.* **2005**, 38, 217–225.
- (9) Meek, S. T.; Greathouse, J. A.; Allendorf, M. D. Metal-Organic Frameworks: A Rapidly Growing Class of Versatile Nanoporous Materials. *Adv. Mater.* **2011**, 23, 249–267.
- (10) Keskin, S.; van Heest, T. M.; Sholl, D. S. Can Metal-Organic Framework Materials Play a Useful Role in Large-Scale Carbon Dioxide Separations? *ChemSusChem* **2010**, *3*, 879–891.
- (11) Park, J.; Howe, J. D.; Sholl, D. S. How Reproducible Are Isotherm Measurement in Metal-Organic Frameworks? *Chem. Mater.* **2017**, *29*, 10487–10495.
- (12) Leperi, K. T.; Chung, Y. G.; You, F.; Snurr, R. Q. Development of a General Evaluation Metric for Rapid Screening of Adsorbent Materials for Postcombustion CO₂ Capture. ACS Sustainable Chem. Eng. 2019, 7, 11529–11539.
- (13) Wilmer, C. E.; Farha, O. K.; Bae, Y. S.; Hupp, J. T.; Snurr, R. Q. Structure-Property Relationships of Porous Materials for Carbon Dioxide Separation and Capture. *Energy Environ. Sci.* **2012**, *5*, 9849–9856.
- (14) Tong, M.; Lan, Y.; Yang, Q.; Zhong, C. High-Throughput Computational Screening and Design of Nanoporous Materials for Methane Storage and Carbon Dioxide Capture. *Green Energy Environ.* **2018**, *3*, 107–119.
- (15) Wiersum, A. D.; Chang, J. S.; Serre, C.; Llewellyn, P. L. An Adsorbent Performance Indicator as a First Step Evaluation of Novel Sorbents for Gas Separations: Application to Metal-Organic Frameworks. *Langmuir* **2013**, *29*, 3301–3309.
- (16) Chung, Y. G.; Gomez-Gualdron, D. A.; Li, P.; Leperi, K. T.; Deria, P.; Zhang, H.; Vermeulen, N. A.; Stoddart, J. F.; You, F.; Hupp, J. T.; Farha, O. K.; Snurr, R. Q. *In silico* Discovery of Metal-Organic Frameworks for Precombustion CO₂ Capture Using a Genetic Algorithm. *Sci. Adv.* **2016**, *2*, No. e1600909.
- (17) Altintas, C.; Erucar, I.; Keskin, S. High-Throughput Computational Screening of the Metal Organic Framework Database for CH₄/H₂ Separations. *ACS Appl. Mater. Interfaces* **2018**, *10*, 3668–3679.
- (18) Sumer, Z.; Keskin, S. Ranking of MOF Adsorbents for CO₂ Separations: A Molecular Simulation Study. *Ind. Eng. Chem. Res.* **2016**, *55*, 10404–10419.

- (19) Altintas, C.; Avci, G.; Daglar, H.; Azar, A. N. V.; Velioglu, S.; Erucar, I.; Keskin, S. Database for CO₂ Separation Performances of MOFs Based on Computational Materials Screening. *ACS Appl. Mater. Interfaces* **2018**, *10*, 17257–17268.
- (20) Braun, E.; Zurhelle, A. F.; Thijssen, W.; Schnell, S. K.; Lin, L. C.; Kim, J.; Thompson, J. A.; Smit, B. High-Throughput Computational Screening of Nanoporous Adsorbents for CO₂ Capture from Natural Gas. *Mol. Syst. Des. Eng.* **2016**, *1*, 175–188.
- (21) Wu, D.; Yang, Q.; Zhong, C.; Liu, D.; Huang, H.; Zhang, W.; Maurin, G. Revealing the Structure-Property Relationships of Metal-Organic Frameworks for CO₂ Capture from Flue Gas. *Langmuir* **2012**, *28*, 12094–12099.
- (22) Keskin, S.; Liu, J.; Rankin, R. B.; Johnson, J. K.; Sholl, D. S. Progress, Opportunities, and Challenges for Applying Atomically Detailed Modeling to Molecular Adsorption and Transport in Metal-Organic Framework Materials. *Ind. Eng. Chem. Res.* **2009**, *48*, 2355–2371.
- (23) Watanabe, T.; Sholl, D. S. Accelerating Applications of Metal-Organic Frameworks for Gas Adsorption and Separation by Computational Screening of Materials. *Langmuir* **2012**, *28*, 14114–14128.
- (24) Maring, B. J.; Webley, P. A. A New Simplified Pressure/Vacuum Swing Adsorption Model for Rapid Adsorbent Screening for CO₂ Capture Applications. *Int. J. Greenhouse Gas Control* **2013**, *15*, 16–31.
- (25) Khurana, M.; Farooq, S. Adsorbent Screening for Post-combustion CO₂ Capture: A Method Relating Equilibrium Isotherm Characteristics to an Optimum Vacuum Swing Adsorption Process Performance. *Ind. Eng. Chem. Res.* **2016**, 55, 2447–2460.
- (26) Balashankar, V. S.; Rajagopalan, A. K.; de Pauw, R.; Avila, A. M.; Rajendran, A. Analysis of a Batch Adsorber Analogue for Rapid Screening of Adsorbents for Postcombustion CO₂ Capture. *Ind. Eng. Chem. Res.* **2019**, *58*, 3314–3328.
- (27) Ga, S.; Jang, H.; Lee, J. H. New Performance Indicators for Adsorbent Evaluation Derived from a Reduced Order Model of an Idealized PSA Process for CO₂ Capture. *Comput. Chem. Eng.* **2017**, *102*, 188–212.
- (28) Danaci, D.; Bui, M.; Dowell, N. M.; Petit, C. Exploring the Limits of Adsorption-Based CO₂ Capture Using MOFs with PVSA from Molecular Design to Process Economics. *Mol. Syst. Des. Eng.* **2020**, DOI: 10.1039/C9ME00102F.
- (29) Bahamon, D.; Diaz-Marquez, A.; Gamallo, P.; Vega, L. F. Energetic Evaluation of Swing Adsorption Processes for CO₂ Capture in Selected MOFs and Zeolites: Effect of Impurities. *Chem. Eng. J.* **2018**, 342, 458–473.
- (30) Nalaparaju, A.; Khurana, M.; Farooq, S.; Karimi, I. A.; Jiang, J. W. CO₂ Capture in Cation-Exchanged Metal-Organic Frameworks: Holistic Modeling from Molecular Simulation to Process Optimization. *Chem. Eng. Sci.* **2015**, *124*, 70–78.
- (31) Faruque Hasan, M. M.; First, E. L.; Floudas, C. A. Cost-Effective CO₂ Capture Based on *in silico* Screening of Zeolites and Process Optimization. *Phys. Chem. Chem. Phys.* **2013**, *15*, 17601–17618.
- (32) Farmahini, A. H.; Krishnamurthy, S.; Friedrich, D.; Brandani, S.; Sarkisov, L. From Crystal to Adsorption Column: Challenges in Multiscale Computational Screening of Materials for Adsorption Separation Processes. *Ind. Eng. Chem. Res.* **2018**, *57*, 15491–15511.
- (33) Rajagopalan, A. K.; Avila, A. M.; Rajendran, A. Do Adsorbent Screening Metrics Predict Process Performance? A Process Optimization Based Study for Post-Combustion Capture of CO₂. *Int. J. Greenhouse Gas Control* **2016**, *46*, 76–85.
- (34) Pullumbi, P.; Brandani, F.; Brandani, S. Gas Separation by Adsorption: Technological Drivers and Opportunities for Improvement. *Curr. Opin. Chem. Eng.* **2019**, 24, 131–142.
- (35) Hasse, D.; Kulkarni, S.; Sanders, E.; Corson, E.; Tranier, J. P. CO₂ Capture by Sub-Ambient Membrane Operation. *Energy Procedia* **2013**, *37*, 993–1003.

- (36) Hasse, D.; Ma, J.; Kulkarni, S.; Terrien, P.; Tranier, J. P.; Sanders, E.; Chaubey, T.; Brumback, J. CO₂ Capture by Cold Membrane Operation. *Energy Procedia* **2014**, *63*, 186–193.
- (37) Liu, L.; Sanders, E. S.; Kulkarni, S. S.; Hasse, D. J.; Koros, W. J. Sub-Ambient Temperature Flue Gas Carbon Dioxide Capture *via* Matrimid® Hollow Fiber Membranes. *J. Membr. Sci.* **2014**, *465*, 49–55.
- (38) Park, J.; Lively, R. P.; Sholl, D. S. Establishing Upper Bounds on CO₂ Swing Capacity in Sub-Ambient Pressure Swing Adsorption *via* Molecular Simulation of Metal-Organic Frameworks. *J. Mater. Chem. A* **2017**, *5*, 12258–12265.
- (39) Agrawal, M.; Sholl, D. S. Effects of Intrinsic Flexibility on Adsorption Properties of Metal-Organic Frameworks at Dilute and Nondilute Loadings. ACS Appl. Mater. Interfaces 2019, 11, 31060—31068.
- (40) Mason, J. A.; Sumida, K.; Herm, Z. R.; Krishna, R.; Long, J. R. Evaluating Metal-Organic Frameworks for Post-Combustion Carbon Dioxide Capture *via* Temperature Swing Adsorption. *Energy Environ. Sci.* **2011**, *4*, 3030–3040.
- (41) Chow, J. C.; Watson, J. G.; Herzog, A.; Benson, S. M.; Hidy, G. M.; Gunter, W. D.; Penkala, S. J.; White, C. M. Separation and Capture of CO₂ from Large Stationary Sources and Sequestration in Geological Formations. *J. Air Waste Manage. Assoc.* **2003**, 53, 1172–1182.
- (42) Granite, E. J.; Pennline, H. W. Photochemical Removal of Mercury from Flue Gas. *Ind. Eng. Chem. Res.* **2002**, *41*, 5470–5476.
- (43) Lee, K. B.; Sircar, S. Removal and Recovery of Compressed CO₂ from Flue Gas by a Novel Thermal Swing Chemisorption Process. *AIChE J.* **2008**, *54*, 2293–2302.
- (44) Sun, W.; Lin, L. C.; Peng, X.; Smit, B. Computational Screening of Porous Metal-Organic Frameworks and Zeolites for the Removal of SO₂ and NO₃ from Flue Gases. *AIChE J.* **2014**, *60*, 2314–2323.
- (45) Burtch, N. C.; Jasuja, H.; Walton, K. S. Water Stability and Adsorption in Metal-Organic Frameworks. *Chem. Rev.* **2014**, *114*, 10575–10612.
- (46) Tang, H.; Fang, H.; Duan, Y.; Sholl, D. S. Predictions of Hg⁰ and HgCl₂ Adsorption Properties in UiO-66 from Flue Gas Using Molecular Simulations. *J. Phys. Chem. C* **2019**, *123*, 5972–2979.
- (47) Hasse, D. J.; Kulkarni, S. S.; Sanders, E. S., Jr.; Tranier, J. P.; Terrien, P. Method of Obtaining Carbon Dioxide From a Carbon Dioxide-Containing Gas Mixture. EP Patent 2,512,634. 2012.
- (48) Garcia, E. J.; Perez-Pellitero, J.; Pirngruber, G. D.; Jallut, C.; Palomino, M.; Rey, F.; Valencia, S. Tuning the Adsorption Properties of Zeolites as Adsorbents for CO₂ Separation: Best Compromise between the Working Capacity and Selectivity. *Ind. Eng. Chem. Res.* **2014**, *53*, 9860–9874.
- (49) Garcia, E. J.; Perez-Pellitero, J.; Pirngruber, G. D.; Jallut, C. Sketching a Portrait of the Optimal Adsorbent for CO₂ Separation by Pressure Swing Adsorption. *Ind. Eng. Chem. Res.* **2017**, *56*, 4818–4829.
- (50) Anderson, R.; Rodgers, J.; Argueta, E.; Biong, A.; Gomez-Gualdron, D. A. Role of Pore Chemistry and Topology in the CO₂ Capture Capabilities of MOFs: From Molecular Simulation to Machine Learning. *Chem. Mater.* **2018**, *30*, 6325–6337.
- (51) Chung, Y. G.; Camp, J.; Haranczyk, M.; Sikora, B. J.; Bury, W.; Krungleviciute, V.; Yildirim, T.; Farha, O. K.; Sholl, D. S.; Snurr, R. Q. Computation-Ready, Experimental Metal-Organic Frameworks: A Tool To Enable High-Throughput Screening of Nanoporous Crystals. *Chem. Mater.* **2014**, *26*, 6185–6192.
- (52) Nazarian, D.; Camp, J. S.; Chung, Y. G.; Snurr, R. Q.; Sholl, D. S. Large-Scale Refinement of Metal-Organic Framework Structures Using Density Functional Theory. *Chem. Mater.* **2017**, *29*, 2521–2528.
- (53) Nazarian, D.; Camp, J. S.; Sholl, D. S. A Comprehensive Set of High-Quality Point Charges for Simulations of Metal-Organic Frameworks. *Chem. Mater.* **2016**, 28, 785–793.
- (54) Rubiera Landa, H. O.; Flockerzi, D.; Seidel-Morgenstern, A. A Method for Efficiently Solving the IAST Equations with an Application to Adsorber Dynamics. *AIChE J.* **2013**, *59*, 1263–1277.

- (55) Walton, K. S.; Sholl, D. S. Predicting Multicomponent Adsorption: 50 Years of the Ideal Adsorbed Solution Theory. *AIChE J.* **2015**, *61*, 2757–2762.
- (56) Dickey, A. N.; Ozgur Yazaydin, A.; Willis, R. R.; Snurr, R. Q. Screening CO_2/N_2 Selectivity in Metal-Organic Frameworks Using Monte Carlo Simulations and Ideal Adsorbed Solution Theory. *Can. J. Chem. Eng.* **2012**, *90*, 825–832.
- (57) Sircar, S. Pressure Swing Adsorption. *Ind. Eng. Chem. Res.* **2002**, 41, 1389–1392.
- (58) Haghpanah, R.; Majumder, A.; Nilam, R.; Rajendran, A.; Farooq, S.; Karimi, I. A.; Amanullah, M. Multiobjective Optimization of a Four-Step Adsorption Process for Postcombustion CO₂ Capture *via* Finite Volume Simulation. *Ind. Eng. Chem. Res.* **2013**, *52*, 4249–4265.
- (59) Ebner, A. D.; Ritter, J. A. State-of-the-art Adsorption and Membrane Separation Processes for Carbon Dioxide Production from Carbon Dioxide Emitting Industries. *Sep. Sci. Technol.* **2009**, *44*, 1273–1421.
- (60) Haghpanah, R.; Nilam, R.; Rajendran, A.; Farooq, S.; Karimi, I. A. Cycle Synthesis and Optimization of a VSA Process for Postcombustion CO₂ Capture. *AIChE J.* **2013**, *59*, 4735–4748.
- (61) Wang, L.; Yang, Y.; Shen, W.; Kong, X.; Li, P.; Yu, J.; Rodrigues, A. E. CO₂ Capture from Flue Gas in an Existing Coal-Fired Power Plant by Two Successive Pilot-Scale VPSA Units. *Ind. Eng. Chem. Res.* **2013**, *52*, 7947–7955.
- (62) Sircar, S.; Hufton, J. R. Why Does the Linear Driving Force Model for Adsorption Kinetics Work? *Adsorption* **2000**, *6*, 137–147.
- (63) Schiesser, W. E. The Numerical Method of Lines: Integration of Partial Differential Equations; Academic Press: San Diego, 1991.
- (64) Vreugdenhil, C. B.; Koren, B. Numerical Methods for Advection-Diffusion Problems: Notes on Numerical Fluid Mechanics; Vieweg: Berlin, 1993.
- (65) Rezaei, F.; Subramanian, S.; Kalyanaraman, J.; Lively, R. P.; Kawajiri, Y.; Realff, M. J. Modeling of Rapid Temperature Swing Adsorption Using Hollow Fiber Sorbents. *Chem. Eng. Sci.* **2014**, *113*, 62–76
- (66) Kalyanaraman, J.; Fan, Y.; Lively, R. P.; Koros, W. J.; Jones, C. W.; Realff, M. J.; Kawajiri, Y. Modeling and Experimental Validation of Carbon Dioxide Sorption on Hollow Fibers Loaded with Silica-Supported Poly(ethylenimine). *Chem. Eng. J.* **2015**, 259, 737–751.
- (67) Fan, Y.; Kalyanaraman, J.; Labreche, Y.; Rezaei, F.; Lively, R. P.; Realff, M. J.; Koros, W. J.; Jones, C. W.; Kawajiri, Y. CO₂ Sorption Performance of Composite Polymer/Aminosilica Hollow Fiber Sorbents: An Experimental and Modeling Study. *Ind. Eng. Chem. Res.* 2015, 54, 1783–1795.
- (68) Lively, R. P.; Chance, R. R.; Kelley, B. T.; Deckman, H. W.; Drese, J. H.; Jones, C. W.; Koros, W. J. Hollow Fiber Adsorbents for CO₂ Removal from Flue Gas. *Ind. Eng. Chem. Res.* **2009**, 48, 7314–7324.
- (69) Lively, R. P.; Chance, R. R.; Mysona, J. A.; Babu, V. P.; Deckman, H. W.; Leta, D. P.; Thomann, H.; Koros, W. J. CO₂ Sorption and Desorption Performance of Thermally Cycled Hollow Fiber Sorbents. *Int. J. Greenhouse Gas Control* **2012**, *10*, 285–294.
- (70) Lively, R. P.; Bessho, N.; Bhandari, D. A.; Kawajiri, Y.; Koros, W. J. Thermally Moderated Hollow Fiber Sorbent Modules in Rapidly Cycled Pressure Swing Adsorption Mode for Hydrogen Purification. *Int. J. Hydrogen Energy* **2012**, *37*, 15227–15240.
- (71) DeWitt, S. J. A.; Sinha, A.; Kalyanaraman, J.; Zhang, F.; Realff, M. J.; Lively, R. P. Critical Comparison of Structured Contactors for Adsorption-Based Gas Separations. *Annu. Rev. Chem. Biomol. Eng.* **2018**, *9*, 129–152.
- (72) Pimentel, B. R.; Fultz, A. W.; Presnell, K. V.; Lively, R. P. Synthesis of Water-Sensitive Metal-Organic Frameworks within Fiber Sorbent Modules. *Ind. Eng. Chem. Res.* **2017**, *56*, 5070–5077.
- (73) Sujan, A. R.; Koh, D. Y.; Zhu, G.; Babu, V. P.; Stephenson, N.; Rosinski, A.; Du, H.; Luo, Y.; Koros, W. J.; Lively, R. P. High-Temperature Activation of Zeolite-Loaded Fiber Sorbents. *Ind. Eng. Chem. Res.* **2018**, *57*, 11757–11766.

- (74) DeWitt, S. J. A.; Rubiera Landa, H. O.; Kawajiri, Y.; Realff, M.; Lively, R. P. Development of Phase-Change-Based Thermally Modulated Fiber Sorbents. *Ind. Eng. Chem. Res.* **2019**, *58*, 5768–5776. (75) Deb, K.; Pratap, A.; Agarwal, S.; Meyarivan, T. A Fast and Elitist Multiobjective Genetic Algorithm: NSGA-II. *IEEE Trans. Evol. Comput.* **2002**, *6*, 182–197.
- (76) Fang, H.; Kulkarni, A.; Kamakoti, P.; Awati, R.; Ravikovitch, P. I.; Sholl, D. S. Identification of High-CO₂-Capacity Cationic Zeolites by Accurate Computational Screening. *Chem. Mater.* **2016**, 28, 3887–3896.
- (77) McDonald, T. M.; Mason, J. A.; Kong, X.; Bloch, E. D.; Gygi, D.; Dani, A.; Crocella, V.; Giordanino, F.; Odoh, S. O.; Drisdell, W. S.; Vlaisavljevich, B.; Dzubak, A. L.; Poloni, R.; Schnell, S. K.; Planas, N.; Lee, K.; Pascal, T.; Wan, L. F.; Prendergast, D.; Neaton, J. B.; Smit, B.; Kortright, J. B.; Gagliardi, L.; Bordiga, S.; Reimer, J. A.; Long, J. R. Cooperative Insertion of CO₂ in Diamine-Appended Metal-Organic Frameworks. *Nature* **2015**, *519*, 303–308.
- (78) Tang, D.; Wu, Y.; Verploegh, R. J.; Sholl, D. S. Efficiently Exploring Adsorption Space to Identify Privileged Adsorbents for Chemical Separations of a Diverse Set of Molecules. *ChemSusChem* **2018**, *11*, 1567–1575.
- (79) Kulkarni, A. R.; Sholl, D. S. Screening of Copper Open Metal Site MOFs for Olefin/Paraffin Separations Using DFT-Derived Force Fields. *J. Phys. Chem. C* **2016**, *120*, 23044–23054.
- (80) Dzubák, A. L.; Lin, L. C.; Kim, J.; Swisher, J. A.; Poloni, R.; Maximoff, S. N.; Smit, B.; Gagliardi, L. *Ab initio* Carbon Capture in Open-Site Metal-Organic Frameworks. *Nat. Chem.* **2012**, *4*, 810–816.
- (81) Poloni, R.; Lee, K.; Berger, R. F.; Smit, B.; Neaton, J. B. Understanding Trends in CO₂ Adsorption in Metal-Organic Frameworks with Open-Metal Sites. *J. Phys. Chem. Lett.* **2014**, *5*, 861–865.
- (82) Woods, M.; Matuszewski, M.; Summers, W. Quality Guidelines for Energy System Studies: CO₂ Impurity Design Parameters. *Tech. Rep. DOE/NETL-341/011212*; US Department of Energy, 2012.
- (83) Agarwal, A.; Biegler, L. T.; Zitney, S. E. A Superstructure-Based Optimal Synthesis of PSA Cycles for Post-Combustion CO₂ Capture. *AIChE J.* **2010**, *56*, 1813–1828.
- (84) Susarla, N.; Haghpanah, R.; Karimi, I. A.; Farooq, S.; Rajendran, A.; Tan, L. S. C.; Lim, J. S. T. Energy and Cost Estimates for Capturing CO₂ from a Dry Flue Gas Using Pressure/Vacuum Swing Adsorption. *Chem. Eng. Res. Des.* **2015**, *102*, 354–367.
- (85) Ko, D.; Siriwardane, R.; Biegler, L. T. Optimization of a Pressure-Swing Adsorption Process Using Zeolite 13X for CO₂ Sequestration. *Ind. Eng. Chem. Res.* **2003**, 42, 339–348.
- (86) Ko, D.; Siriwardane, R.; Biegler, L. T. Optimization of Pressure Swing Adsorption and Fractionated Vacuum Pressure Swing Adsorption Processes for CO₂ Capture. *Ind. Eng. Chem. Res.* **2005**, 44, 8084–8094.
- (87) Nikolaidis, G. N.; Kikkinides, E. S.; Georgiadis, M. C. Model-Based Approach for the Evaluation of Materials and Processes for Post-Combustion Carbon Dioxide Capture from Flue Gas by PSA/VSA Processes. *Ind. Eng. Chem. Res.* **2016**, *55*, 635–646.
- (88) Piantadosi, J.; Howlett, P.; Boland, J. Matching the Grade Correlation Coefficient Using a Copula with Maximum Disorder. *J. Ind. Manag. Optim.* **2007**, *3*, 305–312.
- (89) Fieller, E. C.; Hartley, H. O.; Pearson, E. S. Tests for Rank Correlation Coefficients. I. *Biometrika* **1957**, *44*, 470–481.
- (90) Realff, M. J. The Logic of Efficiency and Other Metrics. J. Adv. Manuf. Process. 2019, 1, No. e10022.
- (91) Walton, K. S.; Sholl, D. S. Research Challenges in Avoiding "Showstoppers" in Developing Materials for Large-Scale Energy Applications. *Joule* **2017**, *1*, 208–211.